Int. J. Electrochem. Sci., 10 **(2015)** 10232 - 10245

International Journal of
ELECTROCHEMICAL
SCIENCE
www.electrochemsci.org

Fabrication of Bioactive Pure Ti by Microarc Oxidation and Hydrothermal Treatment Methods

Chun-Chieh Tseng[1], *Jeou-Long Lee*[2,*]

[1]Medical Device Section, Medical Devices and Opto-Electronics Equipment Department, Metal Industries Research & Development Centre, Kaohsiung 802, Taiwan, R.O.C.
[2]Department of Chemical and Material Engineering, LungHwa University of Science and Technology, Taoyuan ,33306,Taiwan, R.O.C.
[*]E-mail: semxrdedx@yahoo.com.tw

Received: 3 September 2015 / *Accepted:* 22 October 2015 / *Published:* 4 November 2015

Microarc oxidation (MAO) coatings with a rich calcium and phosphorus composition are prepared on the titanium surface in $Ca^{2+}$and PO_4^{3-} ion electrolytes; the surface is then treated with a hydrothermal method in order to obtain the hydroxyapatite (HA). The effects of the different voltage of MAO and hydrothermal treatment (neutral water used) on the surface morphology, phase composition, properties of the coatings and biologically active property are investigated. The results show that the MAO coatings are composed mainly of anatase TiO_2 and that the pore size, surface roughness, thickness, hydrophilic property and corrosion resistance of the MAO coatings strongly depend on the voltage. Furthermore, the proportion of anatase and rutile TiO_2, content of HA and cell proliferation are affected by the hydrothermal treatment (neutral water used). As a result, the MAO and hydrothermal treatment coatings obtain a better hydrophilic property, richer calcium and phosphorus content, favored higher cell proliferation. The oxide films on titanium are characterized by X-ray diffraction (XRD), scanning electron microscopy (SEM), thickness gauge and polarization curves, respectively. In addition, the methyl thiazole tetrazolium (MTT) assay is used to explore the cell proliferation assay.

Keywords: microarc oxidation, titanium, hydrothermal

1. INTRODUCTION

Titanium (Ti) and its alloy have been widely used in dental implants because of its excellent mechanical properties and biocompatibility[1, 2]. However, poor bioactivity, ion release after implantation and weak adhesion with bone tissue has restricted extensive applications and development of titanium and its alloy in the biomedical industry. Surface roughening or coating with bioactive materials could improve the structure of the titanium surface and increase its practical use in

applications. Although biocompatibility of pure titanium is less excellent than of Ti6Al4V, pure titanium has lower cost and is more suitable for machine process. The bioactive calcium phosphate (Ca-P) and hydroxyapatite (HA) are most commonly used as a coating for titanium, and it has been repeatedly demonstrated clinically to have osteoconductive properties after implantation due to its chemical similarity to bone minerals [3, 4]. Therefore, Ca-P or HA-coated Ti implants enhance rapid bone formation because of their osteoconductive property, as compared with uncoated implants. Several methods, such as plasma spraying [5], alkali treatment [6], electrophoresis [7] and anodic oxidation [8], are used to fabricate Ca-P or HA film on the implant. Although these methods are universally used, a few problems, such as low adhesive strength between the coating and substrate and significant biodegradation, have not yet been solved [9, 10]

Microarc oxidation (MAO) is one of the most applicable methods featuring in depositing a hard, porous and adhesive ceramic coating on the surface of Al, Mg or Ti and their alloys [11-12]. It can effectively increase wear resistance, corrosion resistance and mechanical strength of Ti surface, and even with excellent bonding strength with the substrate [13-14]. In recent years, a new method by use of microarc oxidation and hydrothermal treatment has been applied to fabricate the bioactive HA layer. MAO with or without hydrothermal treatment can both be used to induce the Ca and P element incorporated MAO-treated oxide layer to HA [15-20]].In general, these reported literatures [19, 20] used the strong alkaline solution to proceed the hydrothermal treatment. In this study, in order to avoiding the structure and composition of MAO coatings affected by strong alkaline solution, we used the neutral water to carry out of hydrothermal treatment.

The principal aim of the present work is to study the methods that could fabricate bioactive coating on the pure Ti by MAO and hydrothermal treatment (neutral water used). The influence of hydrothermal treatment on the phase structure, surface roughness, corrosion and bioactivity (cell proliferation assay) of MAO coatings were observed. Additionally, the working voltage effect on the properties of MAO coating was also discussed.

2. MATERIAL AND METHODS

Rectangular samples ($50\times25\times2$ mm^3) of pure Ti(grade 4) were used as the substrates for MAO. Prior to the coating, samples were polished with abrasive paper (#2000), degreased with acetone and rinsed with distilled water. The MAO treatment device consisted of a potential adjustable DC power supply up to 1000 V, a 4 liter stainless steel container used as an electrolyte cell, a stirring system and a cooling system [12]. The stainless steel container and the Ti samples were used as cathode and anode, respectively. The electrolyte was prepared from a solution of 10 g/L calcium acetate, 5 g/L sodium dihydrogen phosphate (NaH_2PO_4), 2 g/L sodium metasilicate and 4 g/L ethylenediaminetetraacetic acid disodium salt (EDTA-2Na) in distilled water. Microarc oxidation processes were carried out under the condition of voltages in the range of 250 to 400 V. After an MAO treatment of 30 min, the coated sample was taken out of the electrolyte, rinsed thoroughly with distilled water and dried at room temperature.

Furthermore, the hydrothermal treatment was carried out as the MAO coating samples were placed in the autoclave, adding in 10 ml neutral deionized water with the pH value of 6.8-7.2 (do not contact with the samples), and treated at 250 °C for 8 hours.

2.2 Coating Characterizations

The crystalline structures and constituent phases of the coatings were examined by X-ray diffraction (XRD, Rigaku-2000 X-ray generator) with Cu Kα radiation (wavelength 0.15405 nm) over a scanning range from 20° to 80°. Field emission scanning electron microscopy (FE-SEM, JOEL JSM-6500 F) was employed to examine the surface morphology of the oxide layer. The surface roughness of the coating's oxide layers was measured by α-Step (ET400A) at 20 different randomly selected locations; the average value was calculated and reported. The thickness of MAO coating was measured by using eddy current thickness gage (CMI-100) and at least nine indentations at different places on the coating surface were measured and averaged. The contact angle of the MAO coating, used as a measure of the variation of hydrophilic property, was measured by a contact angle meter (FACE-KYOWA, CA-X) and averaged value of 5 points measured in the surface of the MAO coating was used.

Potentiodynamic polarization tests were carried out in a three-electrode cell system in which a platinum sheet and an Ag/AgCl electrode (0.197 V vs. SHE) were used as the counter and reference electrodes, respectively. The corrosion behavior of all coatings was tested in SBF solutions (SBF :simulated body fluid that is Hanks' balanced salt solution, composed as NaCl 8 g/L, D-Glucose 1g/L, $NaHCO_3$ 0.35 g/L, KCl 0.4 g/L, $CaCl_2 \cdot 2H_2O$ 0.185 g/L, $MgSO_4$ 0.09767, KH_2PO_4 0.06 g/L,$Na_2HPO_4$0.04788 g/L).

All experiments were performed by use of an Autolab PGSTAT30 potentiostat/galvanostat controlled by the GPES (General Purpose Electrochemical System) software. The linear polarization curves were measured in the potential range between −1.25 V and 2.3 V (vs. Ag/AgCl), with a scanning rate of 0.5 mV/s. Before the tests, all specimens were degreased and rinsed with deionized water. All the experiments were carried out at a room temperature of 25±3°C and a relative humidity of 55%±5%.

2.3 Bioactivity test (MTT activity assay)

Cell viability and proliferation were conducted for one day, four days and seven days, respectively and an MTT (3 – (4, 5 – cimethylthiazol-2-yl) -2, 5-diphenyl tetrazolium bromide, REF 11465 007 001, Roche, USA) cell activity assay was carried out. Osteoblast-like cells (MG63), widely used in osteoblast research, (1×10^4 cell/well) were cultured in a 96-well plate. After incubation, the supernatant of each well and cell were removed by means of a phosphate buffered solution (PBS). After incubation for another 4 h, the resultant formazan crystals were dissolved in 0.25 mg/mL thiazolyl blue tetrazolium bromide (SIGMA M5655). Finally, the resultant formazan crystals were dissolved in dimethyl sulfoxid (600 μl) and the absorbance at 540 nm is used to determine optical density (OD) values by an ELISA reader (Stat Fax-2100, Awareness Technology, Inc., Pasadena, CA).

3. RESULTS AND DISCUSSION

3.1 Characteristics of MAO coatings

The variations of surface morphology by the MAO process on titanium are illustrated in Fig. 1. As shown in Figs. 1(a)-(d), there were many micropores and microcracks on the MAO coating surfaces. When the potential was greater than 300 V, the presence of discharge channels could be clearly seen in the micrographs, appearing as dark circular spots distributed all over the surface of the coatings. For voltages of 300, 350 and 400 V, the number of the channels microporous decreased and the discharge channel microporous diameter increased with increasing voltage [21]. The increasing voltage led to an increase in the coating thickness. Figures 1(e)-(h) show the cross sections of the MAO coatings formed at the different voltages. In the thicker layer of oxide coating formed at a higher voltage, more energy was required for the current to pass through the coating. Under this condition, the current was localized at weak points of the layer formed to find its way through the coating. Consequently, the diameter of the discharge channel increased.

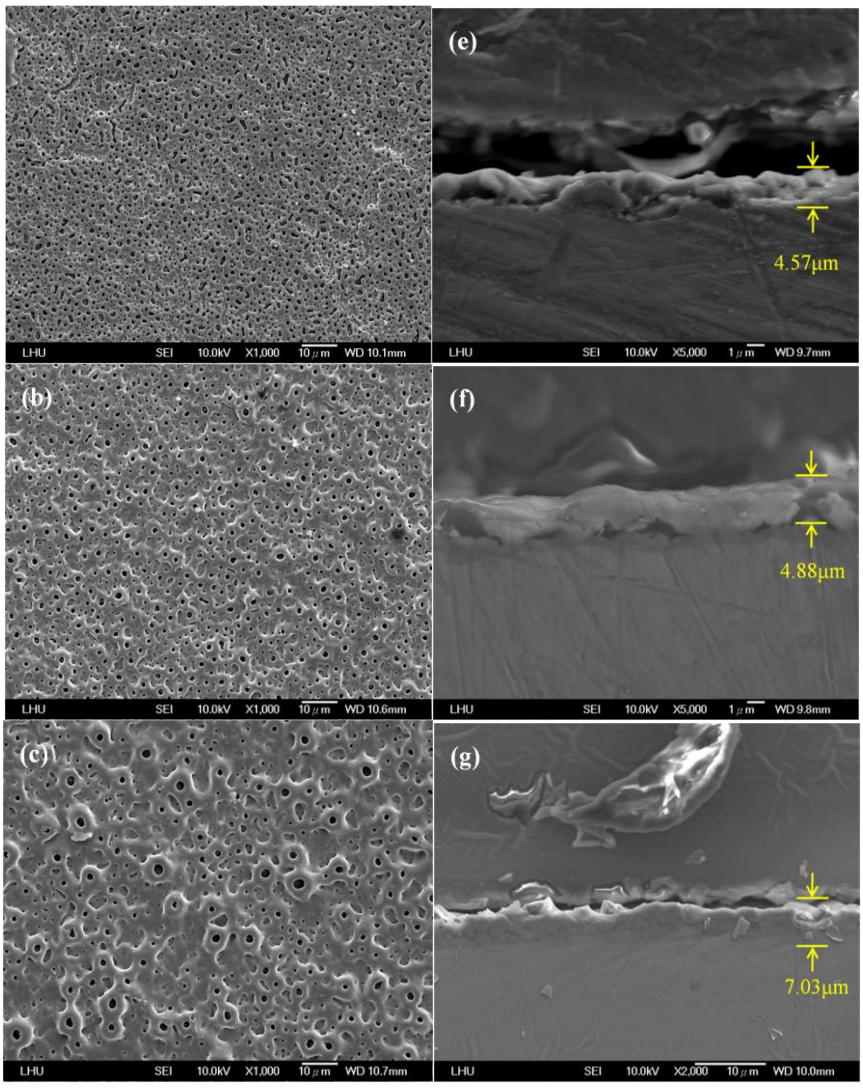

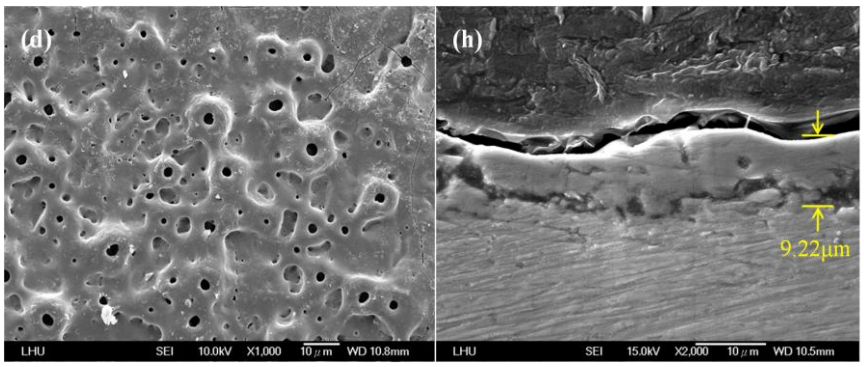

Figure 1. SEM micrographs of MAO coatings of titanium under voltages of MAO coating formed (a) 250, (b) 300, (c) 350 and (d) 400 V; and cross sections (e)~(h)

As shown in Fig. 2, the thickness of MAO coatings formed at 250, 300, 350 and 400 V were 4.57, 4.88, 7.03 and 9.22 μm, respectively, which indicated that a higher voltage could increase the coating thickness. It is known and reported in many papers that the coating growth results from molten titanium oxidized when flowing out through the discharge channels and that its growth rate is almost proportional to the applied voltage [22, 23]. Consequently, the MAO reaction with a higher voltage condition exhibited a higher coating growth rate. Additionally, Fig. 2 also shows that the surface roughness of the oxide coatings increased from 0.5 to 1.6 μm as the voltage increased from 250 to 400 V. In other words, the surface roughness (Ra) in thicker films is higher than that in thinner films. The surface roughness of the coatings was consistent with the observation of the surface morphologies, and this observation is in good agreement with an earlier study [23].

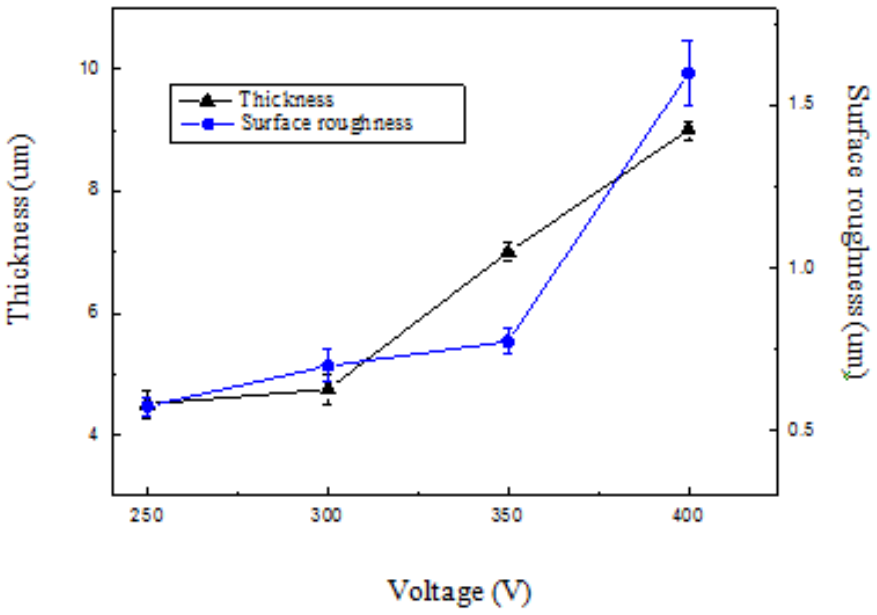

Figure 2. Variations in surface roughness and thickness with MAO coatings of titanium under different voltages of MAO coating formed

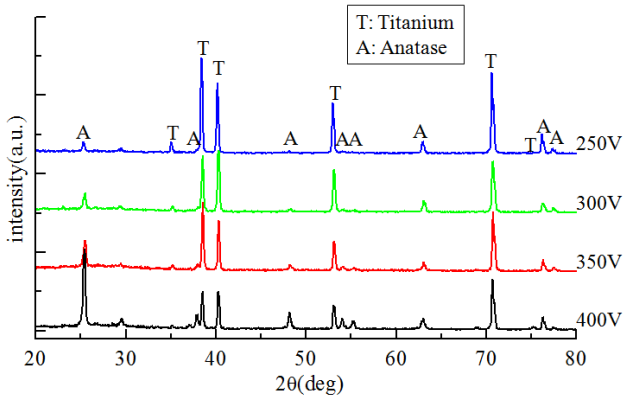

Figure 3. XRD patterns of MAO coatings of titanium under different voltages of MAO coating formed

Fig. 3 shows the XRD patterns of MAO coatings of titanium under voltages of 250, 300, 350, and 400 V. All coatings produced by MAO processing are composed of titanium, and anatase of TiO_2 phases. Usually the composition of the layer is anatase and rutile [24]. But in the Fig.3, the rutile phase does not appear which could be due to the high energy. The XRD results indicated that the content of anatase of TiO_2 increased with increasing voltage. The MAO coatings are formed at high voltages that supply higher energy to the surface, which could play a role in heat treatment and promote the crystallization of amorphous metal oxides.

The anticorrosion behaviors of the Ti substrate and MAO coatings of titanium under voltages of 250, 300, 350 and 400 V were evaluated by potentiodynamic polarization in low corrosion SBF solutions instead of NaCl solution as usual, which were similar to body tissue solution. In a typical polarization curve, a lower corrosion current density corresponds to a lower corrosion rate and better corrosion resistance of the coating. The obtained potentiodynamic polarization curves are shown in Fig. 4.

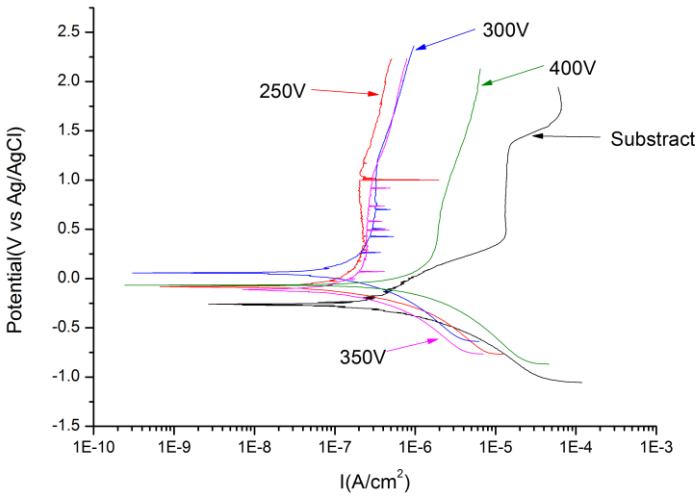

Figure 4. Polarization curve of (a) bare Ti substrate and the polarization curves of MAO coatings formed under voltages of 250, 300,350 and 400 V, respectively

Based on measured from the voltammogram (Fig.4) and Tafel slopes[25], the corrosion current densities (Icorr) and corrosion potential E(i=0) of the MAO coatings formed under different voltages were shown at table 1. The corrosion current densities (Icorr) of the MAO coatings formed under different voltages were shown at table 1. All Icorr data of the MAO coating formed under different voltages are smaller than that of bare Ti substrate; especially, the Icorr of the MAO coating at voltage of 250 V was an order of magnitude lower than that of bare Ti substrate. This is due to the formation of a very dense insulated barrier layer by MAO treatment has less porosity and better corrosion resistance. Furthermore, it is obvious that the corrosion current density increased with voltage.

Otherwise, as mentioned above, both coating thickness and surface roughness increased with the increase of voltage. It was interesting to notice that the much thicker MAO coating formed under voltage of 300, 350 and 400 V showed less corrosion protection than the coating formed under a current density of 250 V. The superior corrosion protection provided by the oxide coating formed under a lower voltage of 250 V could be attributed to this coating having smaller micropores and fewer microcracks, as well as a relatively uniform structure. By contrast with the oxide coating formed under lower voltage, there were more structural imperfections, such as unsealed large micropores and higher porosity on the surface, for the oxide coatings formed under higher voltage. This indicated that the defect density was the dominating influence of corrosion resistance rather than the coating thickness.

Table 1. Comparison of the electrochemical parameters (Ecorr and Icorr) of potentiodynamic polarization curves recorded in SBF solution for bare Ti substrate and MAO coatings under different voltages of MAO coating formed.

Voltage (V)	Icorr (A/cm^2)	Ecorr(V vs. Ag/AgCl)
0 (substrate)	$1.67x10^{-7}$	-0.24207
250	$1.16x10^{-8}$	-0.09385
300	$1.58x10^{-8}$	0.06677
350	$3.72x10^{-8}$	-0.95244
400	$8.25x10^{-8}$	-0.05725

3.2 Effect of hydrothermal treatment

As Fig. 5 shows the XRD pattern of MAO coatings under voltages of 350 and 400 V before and after hydrothermal treatment (neutral water used), the diffraction peaks of hydroxyapatite and calcium pyrophosphate (CPP, $Ca_2P_2O_7$) could be observed though hydrothermal treatment (350V-HT and 400V-HT) for containing Ca-P ions in the titanium oxide layer crystallized into HA [18-21,26] . With a further increase of voltage to 400 V, the content of the hydroxyapatite phase increased after hydrothermal treatment. Therefore, the following probable equations show the reaction of the HA formation during the hydrothermal process.

First, some of $H_2PO_4^-$ ions from surface migrate inward through the discharge channels and decomposed owing to high temperature and pressure by the following chemical reaction[27]:

$$H_2PO_4^- + OH^- = HPO_4^{2-} + H_2O \quad (1)$$

And then, the water in the steam is reduced according to the following equation:

$H_2O = H^+ + OH^-$ (2)

Finally, the HA formation reaction could be proceeded as following equation [27]:

$10Ca^{2+} + 10HPO_4^{2-} + 12OH^- = Ca_{10}(PO_4)_6(OH)_2 + 4PO_4^{3-} + 10H_2O$ (3)

Moreover, the diffraction peaks of CPP composition was formed because the neutral water weak dissociation was insufficient to provide the enough hydroxyl ions to attend the reaction. Therefore, the possible reaction is as following equation:

$2Ca^{2+} + 2HPO_4^{2-} \leftrightarrow Ca_2P_2O_7 + H_2O$ (4)

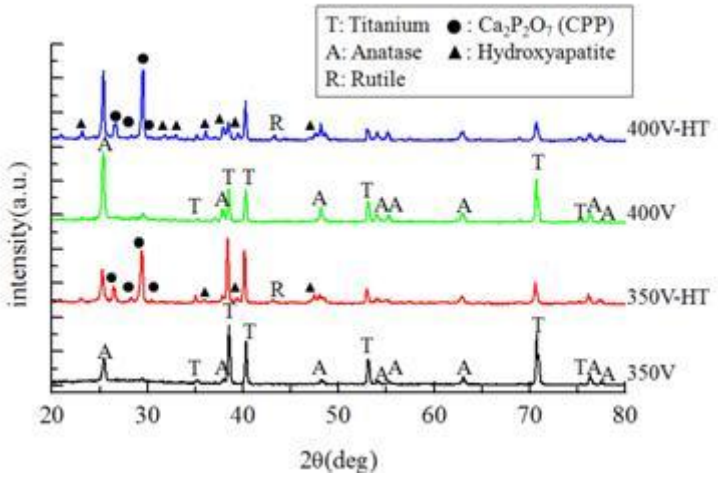

Figure 5. XRD patterns of MAO coatings of titanium under different voltages of MAO coating formed before and after hydrothermal treatment(HT)

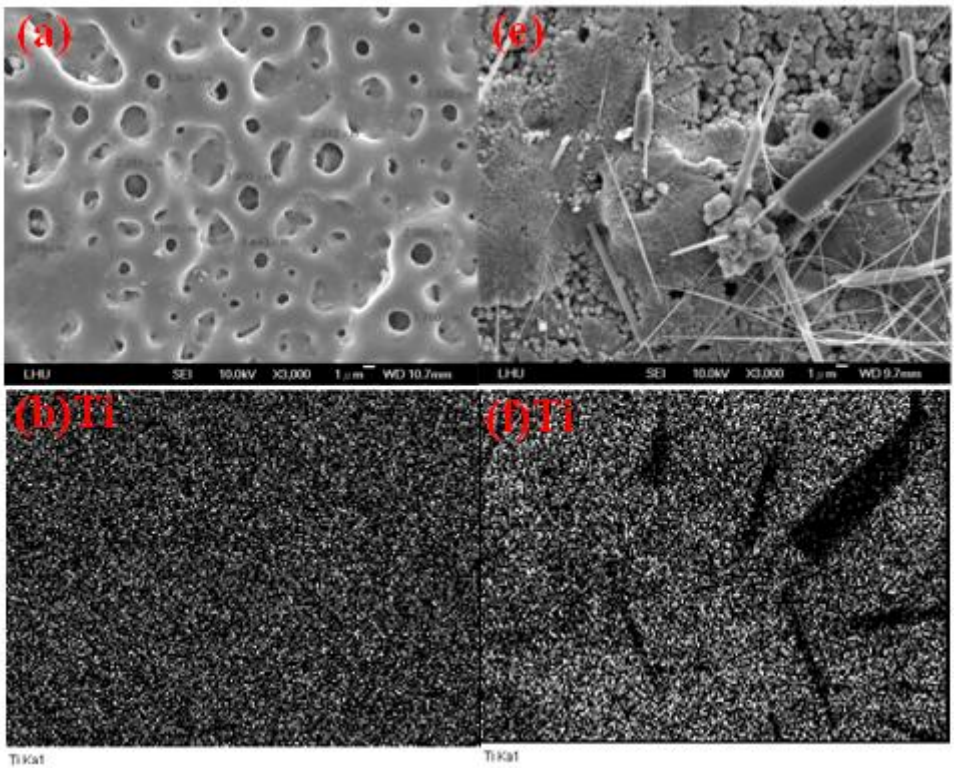

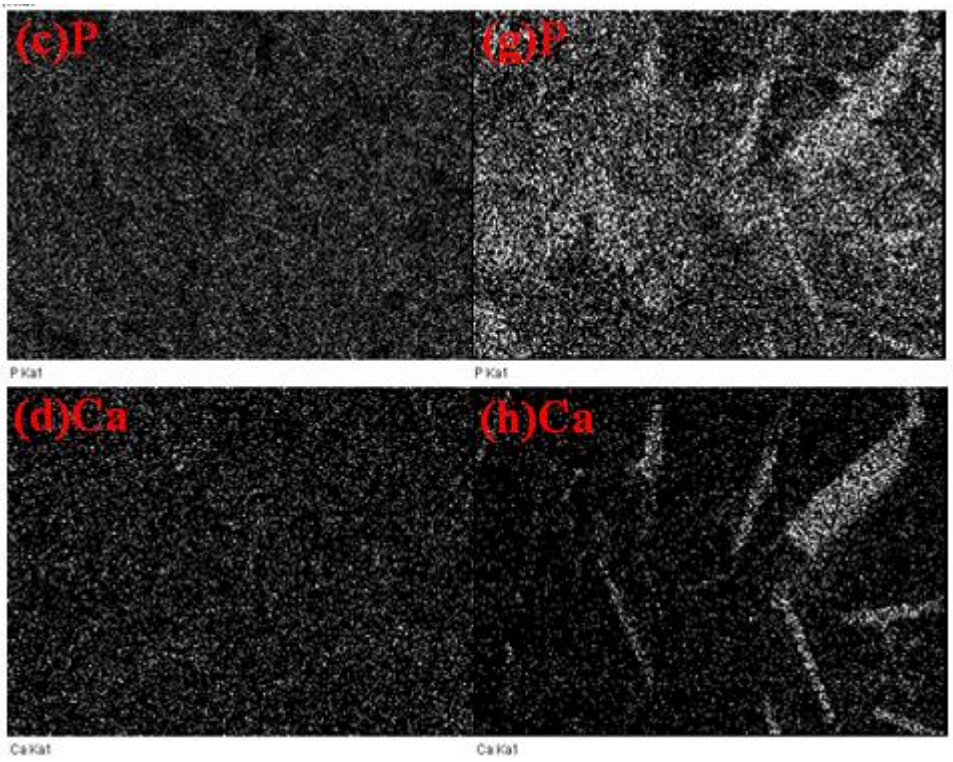

Figure 6. SEM micrographs of MAO coatings of titanium under voltages (350 V) of MAO coating formed (a)without and (e)with hydrothermal treatment; (b-d) for mapping of (a), indicating the quantity of Ti (b), P(c) and Ca(d) elements respectively, (f-h) for mapping of (b), indicating the quantity of Ti (f), P(g) and Ca(h) elements, respectively.

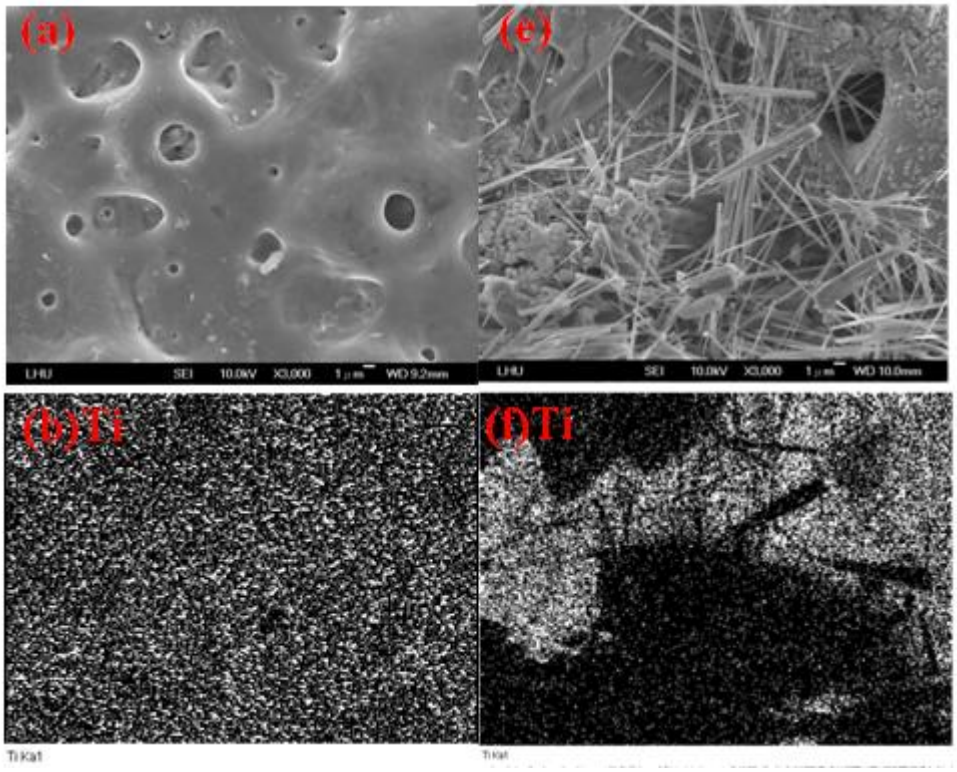

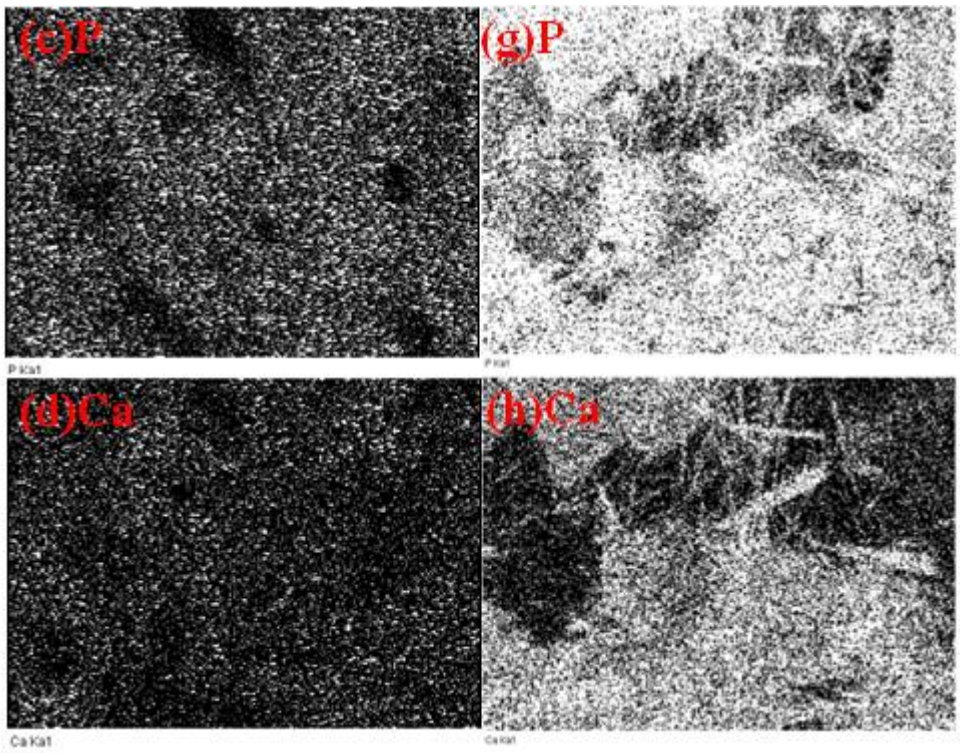

Figure 7. SEM micrographs of MAO coatings of titanium under voltages (400 V) of MAO coating formed (a)without and (e)with hydrothermal treatment; (b-d) for mapping of (a), indicating the quantity of Ti (b), P(c) and Ca(d) elements respectively, (f-h) for mapping of (b), indicating the quantity of Ti (f), P(g) and Ca(h) elements, respectively.

Fig. 6 and Fig.7 show typical SEM images and mappings of MAO coatings of titanium for 30 min under voltages of 350 and 400 V before and after hydrothermal treatment. The SEM images appear the two crystalline phases of hydroxyapatite and anatase of TiO_2 phases. It can be seen from Fig.6 (e) and Fig.7(e) that a needle-like microstructure with a dimension in the range of 5~10 μm and a length in the range of 30~100 μm was obtained. Fig. 6(b-d), Fig. 6(f-h), Fig.7(b-d) and Fig. 7(f-h) show the SEM image mapping for a voltage of 350 and 400 V before(left) and after (right) hydrothermal treatment respectively.

It can be seen from light spots on the mappings that the content of P and Ca were increased, in other words, the Ca and P ions were induced toward the surface of coatings after hydrothermal treatment.

Fig. 8 and 9 show the typical data for the relation between the contact angle θ of MAO coating with the voltage. It can be seen that the contact angle decreases with increasing voltage. This result is in good agreement with an earlier study [28]. As can be seen clearly, the θ of the MAO coating before and after hydrothermal treatment varied sharply from approximately 36.6° to about 5°, it indicated that the surface of MAO coating after hydrothermal treatment had better hydrophilic property and favored cell growth on the surface.

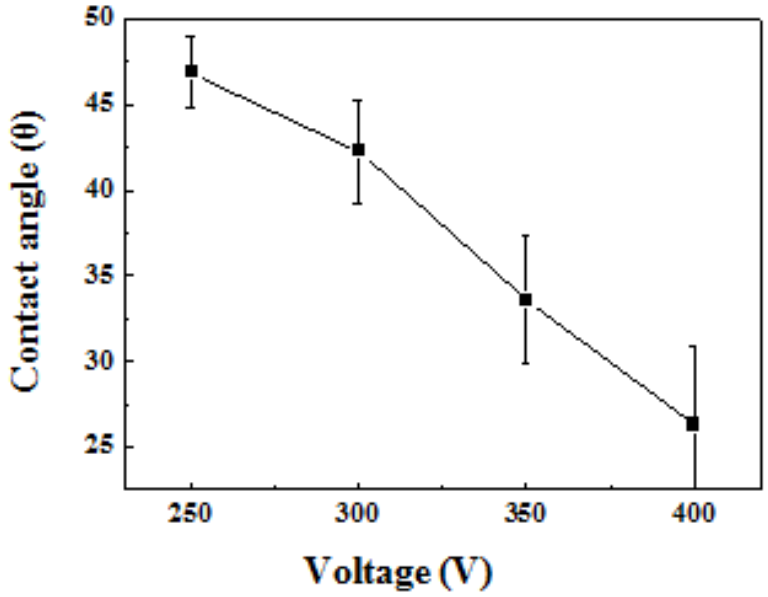

Figure 8 .Variation of contact angle θ with voltage of MAO coating formed

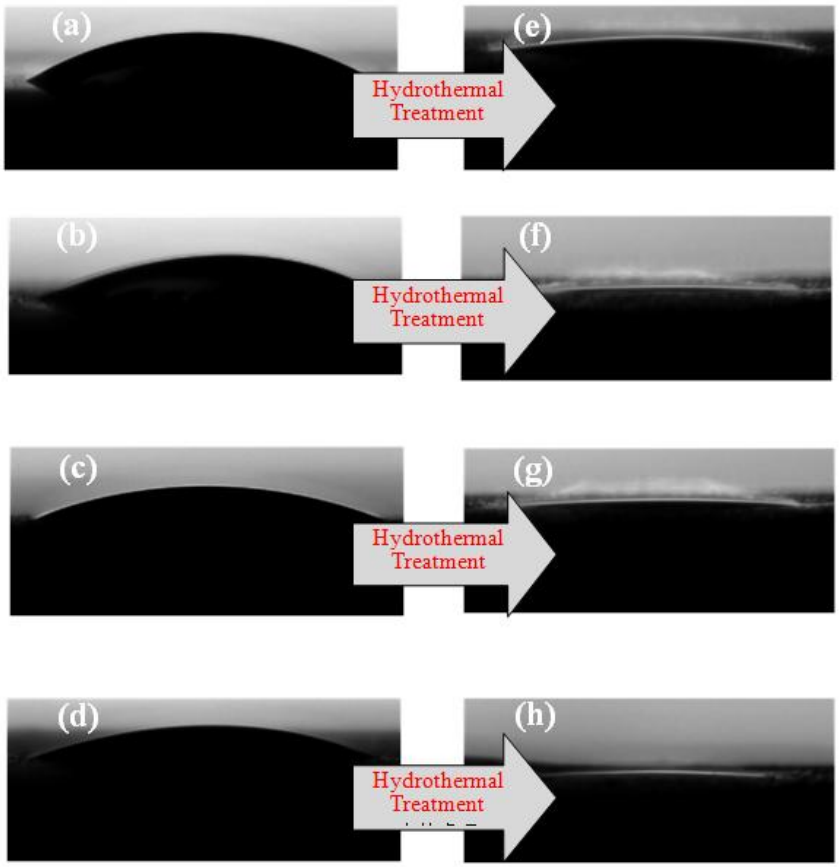

Figure 9. Typical photograph of contact angle test of MAO coating surface at different voltage (250, 300, 350, 400 V) of MAO coating formed: (a-d) of MAO treatment only (; (e-h) for MAO and hydrothermal treatments, respectively.

3.3 Bioactivity test

The MTT activity of the osteoblast-like cell, the uncoated, the MAO-coated and the MAO-coated followed by hydrothermal treatment specimens after incubation for 1, 4, and 7 days is shown in Figure 10. It can be seen that the MTT activities (OD values) on the TiO_2 specimen coated by MAO (under 350V and 400V respectively) followed by hydrothermal treatment were 3-4 times higher than that on the TiO_2 specimen coated by MAO only, and even 6-7 times higher than that on pure Ti substrate.

It has been indicated that the bioactivity property of the Ti implant is influenced by many properties of biomaterials, including surface morphology, composition, hydrophilicity and roughness [17, 29]. Especially, the quantity of osteoconductive properties (as HA, containing compounds of Ca and P, etc.) had played a dominant factor. Therefore, based on the experimental results, the specimen containing rich HA by using hydrothermal treatment, with better hydrophilicity simultaneously, exhibited the greater proliferation of the osteoblast.

Furthermore, the result was indicated that the coating fabricated under higher voltage 400 V, had greater proliferation of the osteoblast than that of voltage 350 V. From former results, the higher voltage had better hydrophilicity and higher roughness. Besides, the surface roughness (1.6μm) of coating fabricated using 400 V was close to the appropriated surface roughness range 2~3μm for osteoblast-like cell growth on the titanium implant [30,31].

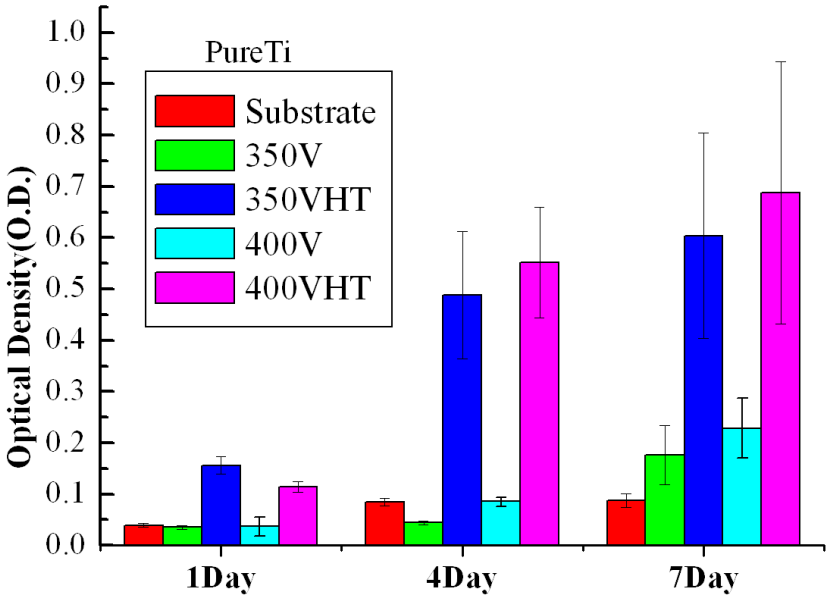

Figure 10. MTT activities of osteoblast-like cells on different treated samples after 1, 4 and 7 days of incubation.

4. CONCLUSION

During the preparation of calcium and phosphorus composition on pure Ti substrate in Ca^{2+} and PO_4^{3-} electrolytes by MAO under different voltage, the surface roughness and thickness of the oxide coatings increased with the voltage. At the same time, the MAO coatings possessed different compositions and microstructures, as well as had better corrosion resistances, as the voltage changed.

Furthermore, the surface of pure Ti after MAO and hydrothermal treatment (neutral water used) obtained better hydrophilicity as well as richer calcium and phosphorus content, including HA and $Ca_2P_2O_7$, and favored cell proliferation. The bioactivities of TiO_2 specimen coated by MAO followed by hydrothermal treatment show 3-4 times higher than that on the TiO_2 specimen coated by MAO only, and even 6-7 times higher than that on pure Ti substrate.

References

1. M.Niinomi, *Mater.Trans.* 49 (2008) 2170.
2. L.H. Li, Y.M. Kong, H.W. Kim, Y.W. Kim, H.Ee. Kim, S.J. Heo, J.Y. Koak, *Biomaterials* 25 (2004) 2867.
3. X. Liu, P.K. Chu and C. Ding, *Mater. Sci. Eng., R.*, 47 (2004)49.
4. L.L. Guehennec, A. Soueidan, P. Layrolle,Y. Amouriq. *Dent. Mater*., 23 (2007) 844.
5. K. Hung, S. Lo, C. Shih, Y. Yang, H. Feng, Y. Lin, *Surf. Coat. Technol*. 231 (2013) 337.
6. G.L.Zhao, L. Xia, B. Zhong, S.S. Wu, L. Song, G.W. Wene, *Trans. Nonferrous Met. Soc. China*, 25(2015) 1151.
7. D.Y. Kim, M. Kim, H.E. Kim,Y.H. Koh, H.W.Kim, J.H. Jang, *Acta Biomater*., 5 (2009) 2196
8. S. Kim, S. Lee, S. Kwak, C. Kim, K. Kim, *Surf. Coat. Technol*. 228 (2013) S37.
9. Z. Zyman, J. Weng, X. Liu, X. Li, X. Zhang, *Biomaterials*, 15 (1994) 151.
10. L.G. Ellies, D.G.A. Nelson, J.D.B. Featherstone, *Biomaterials*, 13 (1992) 313.
11. F.Y. Teng, I.C. Tai, M.W. Wang, Y.J. Wang, C.C. Hung,C.C. Tseng, *J,Taiwan Inst. Chem. Eng*. 45 (2014) 1331.
12. C.C. Tseng , J.L. Lee, T.H. Kuo , S.N. Kuo, K.H. Tseng, *Surf. Coat. Technol.* 206 (2012) 3437.
13. Y. Wang, H. Yu, C. Chen, Z. Zhao, *Mater. Des.*, 85 (2015) 640.
14. H. Wu, X. Lu, B. Long, X. Wang, J. Wang, Z. Jin, *Mater. Lett*,. 59 (2005) 370.
15. A. Lugovskoy, S. Lugovskoy, *Mater. Sci. Eng., C*, 43 (2014) 527.
16. C.J. Hu, J.R. Lu, *Int. J. Electrochem. Sci.*, 10 (2015) 749.
17. Y. Huang, Y.Wang, C. Ning, K. Nan, Y. Han, *Biomed Mater*.,2 (2007) 196.
18. J.H. Ni, Y.L. Shi, F.Y. Yan, J.Z. Chen, L. Wang, *Mater. Res. Bull.*, 43 (2008) 45.
19. A. Alsaran, G. Purcekb, I. Hacisalihogluc, Y. Vangolua, Ö. Bayraka, I. Karamand, A. Celik, *Surf. Coat. Technol.*, 205 (2011) S537;
20. F. Liu, Y. Song, F. Wang, T. Shimizu, K. Igarashi, L.C. Zhao, *J. Biosci. Bioeng.* 100 (2005) 100.
21. P. Huang,Y. Zhang, K. Xu,Y. Han, *J. Biomed. Mater. Res.: Appl. Biomater*.,70 (2004) 187.
22. A.L. Yerokhin, X. Nie, A. Leyland, A. Matthews, *Surf. Coat. Technol*., 130 (2000) 195.
23. L.H. Li, Y.M. Kong, H.W. Kim, Y.W. Kim, H.E. Kim, S.J. Heo, J.Y. Koak, *Biomaterials*, 25 (2004) 2867.
24. P. Huang, F. Wang, K. Xu,Y. Han, *Surf. Coat. Technol.*, 201 (2007) 5168.
25. A. Voicu, N. Duţeanu, A. Răduţă, Ni Vaszilcsin, *Int. J. Electrochem. Sci.*,10 (2015) 5624.
26. X.H. Zhu, C.Z. Wang, B.D. Kou, X.K. Su, W.Q.Zhang, *Trans.Mater.Heat Treat.,Proc.14th Ifhtse Congr.*, 25 (2004) 1064.
27. L.Y. Huang, K.W. Xu,J. Lu, *J. Mater. Sci. Mater. Med.*, 11 (2000) 667.

28. M.R. Bayati, R. Molaei, A. Kajbafvala, S. Zanganeh, H.R. Zargar, K. Janghorban, *Electrochim. Acta*, 55 (2010) 5786.
29. L. Le Guéhennec, A. Soueidan, P. Layrolle, Y. Amouriq, *Dent. Mater.*,23 (2007) 844.
30. J. Lincks, B.D. Boyan, C.R. Blanchard, C.H. Lohmann, Y. Liu, D.L. Cochran, D.D. Dean, Z. Schwartz, *Biomaterial*s,19 (1998) 2219.
31. M.J. Kim, M.U. Choi,C.W. Kim, *Biomaterials*, 27 (2006) 5502.